# A DFT Study of Hydrogen Dissociation on CO- and C-Precovered Fe(100) Surfaces

**Eric van Steen and Pieter van Helden***

*Centre for Catalysis Research, Department of Chemical Engineering, University of Cape Town, Private Bag X3, Rondebosch, 7701, South Africa*

*Received: October 9, 2009; Revised Manuscript Received: January 20, 2010*

A DFT model of the Fe(100) surface was used to study the dissociation process of $H_2$. The dissociation of $H_2$ was considered on a clean surface as well as CO- and C-precovered surfaces. The presence of CO and C is shown to block several sites for hydrogen adsorption, as well as increasing various hydrogen dissociation barriers. At CO and C coverages up to 0.25 ML the main contributor to the barrier increase is the CO−H and C−H repulsion. In these cases, off-symmetry sites will play an important role in the dissociation of the approaching hydrogen molecules. At coverages of 0.5 ML of CO and C, adsorption site blocking occurred, and the dissociation barriers increased to more than 3 times larger values than that of the clean surface. This increase in the barriers will result in a significant decrease in the rate constant of the dissociative $H_2$ adsorption process.

## Introduction

Studies of the process of hydrogen adsorption on iron surfaces have been motivated by the importance of this process in the field of heterogeneous catalysis. This is the case, since hydrogen adsorption is one of the first reactions in the representation of various catalytic cycles. This can further be seen in its particular application in the ammonia synthesis[1] and Fischer−Tropsch synthesis reactions.[2]

Although the hydrogen dissociation reaction seems to be a simple reaction, it has quite a lot of intricacies. In the first step of the process of hydrogen chemisorption on a metal surface, the $H_2$ molecule approaches the surface. As this happens the electrons in the filled $1\sigma_g$ orbital start to overlap with the filled orbitals of the metal surface, resulting in a Pauli repulsion with the accompanying increase in energy. As the $H_2$ comes even closer, the empty antibonding $1\sigma_u$* orbital becomes partially occupied, weakening the H−H bond slightly. As all of this happens, new strong chemical bonds with the surface start to form which also counteracts the Pauli repulsion. The specific point at which this counteraction takes place determines the position of the barrier on the hydrogen adsorption potential energy surface (PES).[3] This interaction of attractive and repulsive potentials will differ at different sites on the metal surface. It will also depend on the orientation of the hydrogen molecule. The dissociation activation energy can therefore differ at various sites. Such a corrugated potential can dynamically "steer" the approaching hydrogen molecule to the more favorable sites for dissociation.[4] Other effects that have been noted to play a role in certain cases are quantum tunnelling and zero-point energy effects.[5]

The study of hydrogen chemisorption on a clean Fe(100) surface has been the focus of a number of studies.[6−10] On the Fe(110), Fe(100), and Fe(111) surfaces, hydrogen undergoes dissociative chemisorption.[6] On the clean Fe(100) two adsorption states, $\beta_1$ and $\beta_2$, have been identified. Temperature programmed desorption (TPD) showed that the $\beta_2$ activation energy of desorption is 23.0 kcal/mol (1.00 eV).[7] The desorption activation energy of $\beta_1$ state has been established as 14.1 kcal/mol (0.74 eV).[8] It was also proposed that the Fe−H bond energy has a lower limit of 59.0 kcal/mol.[7] From theoretical work it has been established that the 4-fold hollow and the bridge sites are available hydrogen adsorption sites with the 4-fold hollow site as the slightly more favorable adsorption site.[9] By use of the PW91 functional, the classical adsorption barrier on the top site was calculated at 3.6 kcal/mol (0.16 eV) and over the bridge site at 3.5 kcal/mol (0.15 eV).[9] From molecular beam experiments the value of the $H_2$ dissociation barrier was estimated at 0.45 eV.[10] In contrast to this, Burke and Madix have proposed an upper limit to the adsorption activation barrier of about 2.0 kcal/mol (0.01 eV), which corresponds to a sticking probability of $s_0 = 0.05$.[7]

This picture might change significantly once other adsorbates are present on the surface. In this regard, Ko and Madix[11] showed that the presence of either carbon or oxygen hindered the dissociative adsorption of hydrogen on Mo(100). When a surface is therefore modified with a preadsorbed species, it can have an effect on the dissociation of hydrogen. Various explanations have been put forward for this type of "poisoning". Feibelman and Hamann[12,13] proposed that this effect is due to an adsorbate-induced change of the Fermi level density of states (DOS). Hammer[14] considered the increase in the $N_2$ adsorption barrier when surface impurities are present as a function of the change in the surface d-band structure due to the preadsorbed species. Nørskov et al.[15] proposed a slightly different model for the poisoning. They proposed that the change in reactivity by an adlayer is due to the interaction of the hydrogen molecule with the electrostatic field that is induced by the adlayer. For dissociative hydrogen adsorption, they predict that electronegative adlayers are usually poisons for hydrogen dissociation and that electropositive adlayers are promoters for hydrogen dissociation.

These models suggest that C and CO adsorbates can be poisons, but they do not give a detailed microscopic description of the hydrogen dissociation process in their presence. Local effects can occur by increased dissociation barriers along specific dissociation pathways of the hydrogen molecule or simply by the blocking of adsorption sites for atomic hydrogen.

* To whom correspondence should be addressed. E-mail: pieter.vanhelden@sasol.com.

10.1021/jp909689a 
Published on Web 03/11/2010

Examples of these effects are the simultaneous blocking of adsorption sites and the increase of dissociation barriers on a sulfur precovered Pd(100) surface.[16] Sulfur can increase the dissociation barrier at low S coverage by changing the Pd electronic structure, but when the hydrogen molecule is less than 1.5 Å away from the S, the main contribution is blocking of the adsorption site due to a strong S−H repulsion.

In this paper, we use density functional theory (DFT) to calculate the potential energy surface (PES) for the $H_2$ dissociation process on the Fe(100) surface. We consider the dissociation process on various high-symmetry sites in the p(2 × 2) surface unit cell on a clean surface. Since two other species that will be present on the surface in the Fischer−Tropsch process are CO and C, we also consider these adsorbate-precovered surfaces at various coverages. In previous work[17] we discussed the adsorption and coadsorption structures and energies of hydorgen and CO. We showed that H and CO will be in a mixed coadsorbed state on the Fe(100) surface if it coadsorbes. In the current work, we present the most important PES profiles and discuss the various effects that play a role in the adsorption of hydrogen on these precovered Fe(100) surfaces.

## Methods and Models

**Calculational Setup.** All the calculations in this study were performed using the CASTEP[18] code. This code employs periodic DFT calculations with a plane wave basis set and pseudopotentials. We used the generalized gradient approximation (GGA) with the Revised Perdew−Burke−Enzerhof (RPBE) functional.[19] The electron distribution at the Fermi level was modeled by a Gaussian smearing method with $\sigma = 0.1$ eV. The ion−electron interactions were described by core-corrected ultrasoft pseudopotentials as included in the CASTEP suite.[20]

A five-layer Fe(100) slab was used with an optimized 17 Å vacuum layer between the surfaces. This large vacuum spacing ensures that the initial hydrogen molecule is sufficiently far away from both surfaces of the Fe slab. The surface was represented by using a p(2 × 2) surface unit cell. The *k*-point sampling was generated by following the Monkhorst−Pack[21] procedure with a 4 × 4 × 1 mesh. The plane wave basis set cutoff energy was set at 400 eV. All the coordinates of the atoms in the slab were fully relaxed before the hydrogen molecule was introduced into the cell. The calculational setup parameters (the *k*-points mesh, the number of slab layers, the vacuum spacing, etc.) were tested and optimized.

We calculated the equilibrium lattice constant for bulk iron at 2.852 Å with a bulk modulus of 176 GPa using the Birch−Murnaghan equation of state.[22,23] A magnetic moment of 2.31 $\mu_B$ per iron atom was also calculated. These values are in good agreement with the experimental values of 2.86 Å, 168 GPa, and 2.24 $\mu_B$.[24,25] The calculated surface energy was 2.36 J m$^{-2}$, which is in good agreement with the experimental value of 2.41 J m$^{-2}$.[26]

The energy and properties of the gas-phase hydrogen molecule were calculated by placing the molecule in a cubic unit cell with 10 Å sides. For $H_2$ we obtained a equilibrium bond distance of $r_e = 0.749$ Å, a vibrational frequency of $\nu = 4421$ cm$^{-1}$, and a dissociation energy of $D_e = 4.56$ eV. These values are in good agreement with the experimental values ($r_e = 0.741$ Å, $\nu = 4401$ cm$^{-1}$, and $D_e = 4.56$ eV).[27]

**Dissociation Model.** The full description of an $H_2$ molecule approaching the surface has six dimensions [*X*, *Y*, and *Z* coordinates of the center of mass, the $H_2$ interatomic distance, and the polar ($\theta$) and azithmuthal ($\phi$) angles of the molecular axis]. To fully calculate this large configurational space will be immensely time-consuming, and therefore we had to simplify our approach. We only considered specific 2D cuts through this 6D surface. The two dimensions under consideration are the $H_2$ interatomic distance and the height of the center of mass above the surface (*Z*). Furthermore, we only consider the orientation of $H_2$ with the $H_2$ bond parallel to the surface, since it has been shown that the "helicopter" rotation of the $H_2$ molecule (molecular axis parallel to the surface) is more favorable for $H_2$ dissociation than the "cartwheel" rotation (out of plane rotation).[4,28−31] Only a direct approach of the $H_2$ (in line with the surface normal) was considered, because generally only the kinetic energy of the normal component of the $H_2$ incidence angle has a significant effect on the sticking probability.[32]

The surface slab geometry was kept fixed for all of the studied $H_2$ adsorption pathways. This approximation can be used since the mass mismatch of H with the Fe atoms is quite large. The reference energy zero is taken as the energy of the geometry, where the hydrogen molecule is 4.00 Å away from the surface. Single point energies were calculated for a large range of possible combinations of the height of the $H_2$ above the surface and the $H_2$ bond length. An interpolation of the energy values was done, resulting in classical "elbow plot" graphs. All isoenergetic lines in these graphs are 0.10 eV apart. Zero-point corrections are not included in the PES, but will be considered separately. The surface slabs containing the adsorbed CO and C were also allowed to relax before the hydrogen molecule was introduced into these cells.

**Zero Point Corrections, DOS, and Charge Analysis.** It is important to consider the effect zero-point energies have on the barrier height, since it has been shown that it is one of the quantum effects for the dissociation of $H_2$.[28] A classical particle can follow the minimum-energy path of a PES exactly. A quantum particle is delocalized and cannot follow the bottom valley of the PES. The minimum energy path of a quantum particle requires the inclusion of at least the zero-point energy perpendicular to the minimum energy pathway.[5] We estimated the minimum zero-point energies for a specific PES by fitting the potential at various points to a Morse potential.[33] From this fit we obtain the anharmonic zero-point vibrational frequency ($\nu_0$) and the potential well depth ($D_e$). These values were used to estimate the minimum zero-point energy, calculated by

$$E_0 = \frac{1}{2}h\nu_0 - \frac{\left(\frac{1}{2}h\nu_0\right)^2}{4D_e} \quad (1)$$

The electronic local density of states (LDOS) was calculated by a projection of the wave functions onto spherical harmonics to obtain the s, p, and d character of the electrons. The DOS is given relative to the Fermi level of each system. All the DOS plots are shown as spin-polarized with the α-spin profile at the top and the $\beta$-spin profile at the bottom. We also estimated the charge of the preadsorbed C and CO on the surface by a Mulliken charge analysis.[34,35]

## Results

We calculated the 2D cuts in the $H_2$ adsorption potential energy surface (PES) for a clean Fe(100) surface, as well as CO and C precovered surfaces. The adsorption potential energy surfaces will be described by following the minimum energy pathway. All PES saddle points (transition states) are noted on the PES profiles with a marker (+). The $H_2$ molecule approaches

**TABLE 1: Summary of the Calculated Barriers for $H_2$ Dissociation on Clean and Precovered Fe(100)**

| profile | site | $E_a$ (eV) | $E_{a,ZPC}$ (eV)[a] | barrier position[b] |
|---|---|---|---|---|
| clean Fe(100) | top | 0.24 | 0.16 | late |
| | top 45° | 0.33 | 0.22 | late |
| | bridge | 0.34 | 0.26 | early |
| | hollow | 0.86 | 0.73 | early |
| $\theta_{CO} = 0.25$ ML | top | 1.46 | 1.34 | late |
| | top 45° | 0.90 | 0.80 | late |
| | bridge | 0.33 | 0.24 | early |
| | off-symm. top 45° | 0.35 | 0.26 | late |
| $\theta_{CO} = 0.50$ ML | top | 2.67 | 2.49 | late |
| | top 45° | 1.33 | 1.24 | late |
| $\theta_{CO,tilted} = 0.50$ ML | top 45° | 2.46 | 2.23 | center |
| $\theta_C = 0.25$ ML | top | 0.55 | 0.46 | late |
| | top 45° | 0.49 | 0.40 | late |
| | bridge | 0.31 | 0.23 | early |
| | off-symm top 45° | 0.25 | 0.08 | late |
| | top C | 2.20 | 2.07 | center |
| $\theta_C = 0.50$ ML | top | 0.95 | 0.84 | late |
| | top 45° | 0.71 | 0.60 | late |

[a] $E_{a,ZPC}$ indicates the zero-point-corrected barrier estimates [b] This indicates the position of the dissociation barrier on the PES.

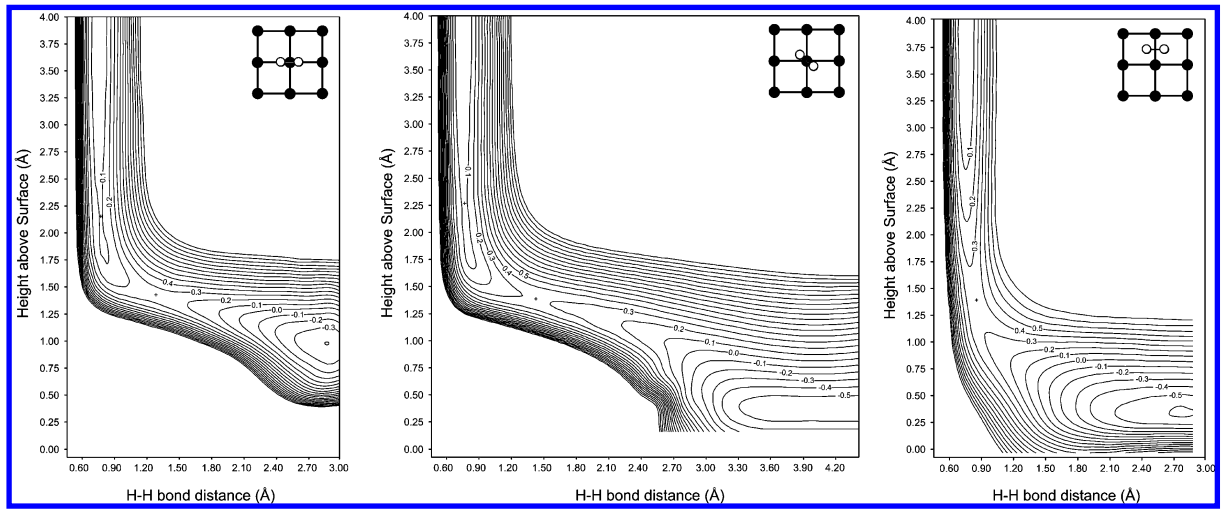


**Figure 1.** PES for $H_2$ dissociation on a clean Fe(100) surface with $H_2$ on top (left), on top rotated by 45° (center), and on the bridge site (right).

the surface from 4 Å above the surface with an equilibrium bond length of 0.794 Å. A summary of all the activation energies is given in Table 1.

**$H_2$ Dissociation on the Clean Fe(100) Surface.** The resulting $H_2$ dissociation profiles on a clean Fe(100) surface can be seen in Figure 1. The left of Figure 1 shows the dissociation profile of $H_2$ on the top site with H atoms ending up on the bridge sites. The $H_2$ approaches to 2.2 Å, where it goes over a small barrier of 0.08 eV to enter a molecular adsorbed state at 1.8 Å above the surface. The H−H bond length is slightly stretched at 0.82 Å. The depth of the energy well of this molecularly adsorbed state is 0.03 eV. This is much smaller than the energy well calculated by Sorescu using the PW91 functional.[9] The simultaneous H−H bond stretch and surface-H bond shortening results in an energy increase up to the dissociation activation energy barrier at 1.42 Å above the surface, with the H-atoms separated at 1.25 Å and with an energy value of about 0.24 eV. This is larger than the barrier calculated by Sorescu for the same site (0.16 eV).[9] After inclusion of the ZPE correction for this profile the height of the dissociation barrier (0.16 eV) compares somewhat better with Sorescu's ZPE corrected value of 0.09 eV. After the barrier the H−H distance increases until the H-atoms are bonded at the bridge site (2.85 Å separation) at a height of 0.95 Å above the surface. The adsorption energy of the two H atoms on the bridge site is −0.41 eV ($E_{ads} = -0.21$ eV per H atom).

The center profile of Figure 1 shows the dissociation profile of $H_2$ on the top site with the H−H bond rotated by 45° in the plane parallel to the surface. In this case, the H atoms end up in the hollow sites. The $H_2$ approaches to 2.2 Å, where it goes over a small barrier of 0.08 eV to enter a molecular adsorbed state at 1.8 Å above the surface with a slightly stretched H−H bond length at 0.81 Å. The depth of the energy well of this molecularly adsorbed state is also 0.03 eV. The dissociation barrier has an energy value of about 0.33 eV. The separation of the H-atoms increases until they are bonded in hollow sites separated at 4.02 Å with a height of 0.30 Å above the surface. The adsorption energy of the two H atoms in these hollow sites is −0.59 eV ($E_{ads} = -0.30$ eV per H atom).

The right profile in Figure 1 shows the dissociation profile of $H_2$ on the bridge site with the H atoms ending up in the hollow sites. The $H_2$ approaches to 1.4 Å, where it reaches a barrier of 0.34 eV with a slightly stretched H−H bond length at 0.85 Å. Only after this barrier the H−H bond starts to stretch significantly until they are both bonded in hollow sites at a height of 0.30 Å above the surface. The adsorption energy of the two H atoms in these hollow sites is −0.62 eV ($E_{ads} = -0.31$ eV per H atom).

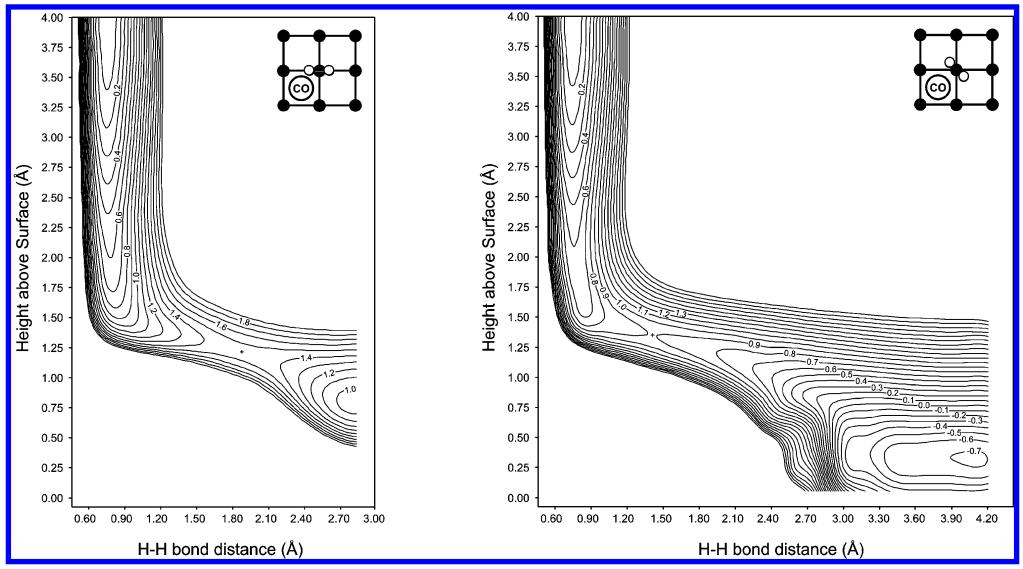


**Figure 2.** PES for $H_2$ dissociation on a $\theta_{CO} = 0.25$ ML precovered Fe(100) surface with $H_2$ adsorption on top (left) and on top rotated by 45° (right).

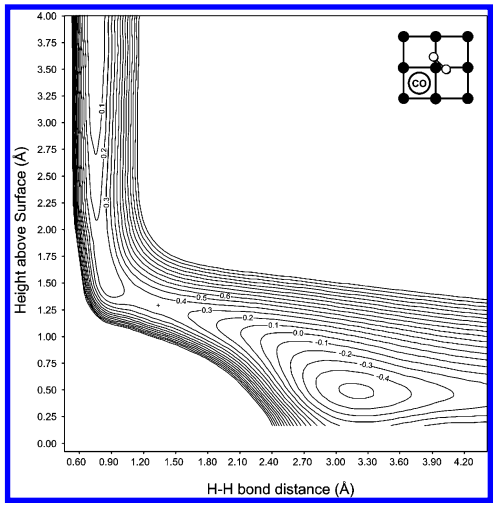


**Figure 3.** PES for $H_2$ dissociation on a $\theta_{CO} = 0.25$ ML precovered Fe(100) surface with $H_2$ rotated by 45°. The $H_2$ center of mass is slightly moved from the high-symmetry top site.

We also considered the dissociation profile of $H_2$ over the hollow site with H atoms ending up on the bridge sites. As the $H_2$ approaches the surface, it experiences a very strong repulsion. The barrier of 0.86 eV is reached at 1.25 Å above the surface with a slightly stretched H−H bond length at 0.83 Å.

**$H_2$ Dissociation on the CO-Covered Fe(100) Surface.** Besides hydrogen, the other component in synthesis gas is CO. We considered the effect of adsorbed CO on the process of hydrogen adsorption by considering CO perpendicularly adsorbed in the hollow site at coverages of $\theta_{CO} = 0.25$ ML and $\theta_{CO} = 0.5$ ML. We consider the same pathways as those described on the clean surface.

***$\theta_{CO} = 0.25$ ML.*** The profiles for $H_2$ dissociation on a $\theta_{CO} = 0.25$ ML precovered surface can be seen in Figures 2 and 3. The left profile of Figure 2 shows the dissociation profile of $H_2$ on the top site with H atoms ending up on the bridge sites. As the $H_2$ approaches the surface, it experiences a much stronger repulsion than what was seen for the corresponding pathway on a clean surface. This is due to the fact that the CO molecule orbitals extend further into the vacuum. These CO orbitals contribute to a strong Pauli repulsion interaction with the $H_2$ at an earlier stage in the $H_2$ approach. No molecular adsorbed state can be observed in this profile. The H−H bond stretches and the surface-H bond shortens with a corresponding increase of the energy to 1.46 eV at the dissociation barrier. After the barrier the H atoms are bonded at the bridge sites. The energy of the two H atoms is 0.94 eV at this point. This is much less stable than gas-phase $H_2$. It is important to keep in mind that in this case the two H atoms are not equivalent. The one that is the closest to the CO molecule would probably experience severe forces that will direct it down to the hollow site right next to it. This would result in a more favorable energetic configuration. At this CO coverage, this seems to be a very unlikely dissociation pathway.

In contrast to the on top site, the dissociation barrier is slightly lower for the on top site with the H−H bond rotated by 45° parallel to the surface plane (right panel of Figure 2). In this case, both the H atoms end up in hollow sites. As the $H_2$ approaches the surface, it once again experiences a strong repulsion. No distinct molecular adsorbed state can be observed. The energy value of this activation barrier is 0.90 eV. This barrier is much higher than on a clean surface, but it is significantly lower than that of the previously considered top-site approach. The H-atoms end up in hollow sites with an adsorption energy for the two H atoms of −0.72 eV ($E_{ads}$ = −0.36 eV per H atom).

From the previous two profiles, it is clear that there is a strong repulsion between the CO and the approaching $H_2$ molecule. We therefore also considered an adsorption profile similar to the on top site with the H−H bond rotated by 45°, but with the $H_2$ center of mass shifted away from the CO by 0.5 Å. We call this the rotated *off-symmetry site*. This profile can be seen in Figure 3. It is clear that the CO−$H_2$ repulsion is significantly smaller here. The initial repulsion is reduced to almost the same level as that of the clean surface. The corresponding dissociation barrier is 0.35 eV. This is in line with that of the clean surface.

We also considered the dissociation of $H_2$ on the bridge site that is not directly next to an adsorbed CO. The H atoms end up in hollow sites. The $H_2$ reaches a barrier of 0.33 eV with a profile that looks exactly like that of the clean surface bridge site. Upon calculation of the dissociation profile over the possible hollow sites, a larger repulsion was experienced than that which was observed on the clean surface, indicating that the barriers will be even higher than that of the clean surface hollow sites.

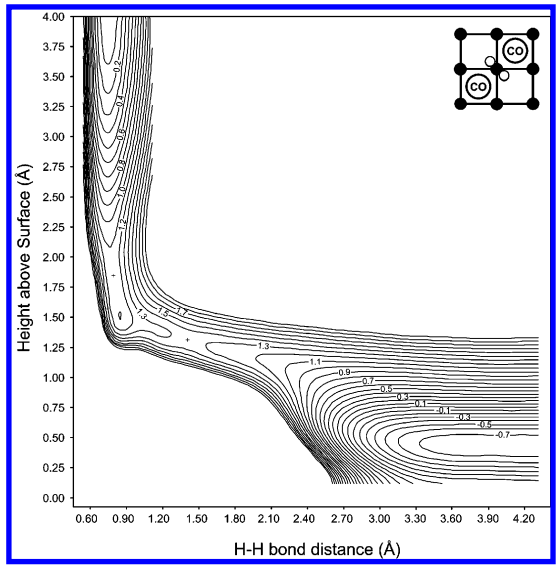


**Figure 4.** PES for $H_2$ dissociation on a $\theta_{CO} = 0.5$ ML precovered Fe(100) surface with $H_2$ on top and on top rotated by 45°.

***$\theta_{CO} = 0.50$ ML.*** At this coverage all of the bridge sites will have a CO molecule in a hollow site next to it. On the basis of the results at $\theta_{CO} = 0.25$ ML, the strong repulsion between CO and $H_2$ can be expected to effectively block these bridge sites for adsorption. The dissociation barrier for a $H_2$ molecule on the top site (with the H atoms ending up on the bridge sites) has an extremely high energy value of 2.67 eV. Similarly dissociation over the hollow sites and bridge sites cannot take place, since these bridge sites are blocked by the adsorbed CO molecules in the hollow sites.

Figure 4 shows the dissociation profile of $H_2$ on the top site with the H−H bond rotated by 45° parallel to the surface plane. In this case, the H atoms end up in the two remaining hollow sites. The initial repulsion $H_2$ experiences as it approaches the surface is similar to that at $\theta_C = 0.25$ ML (see below). The calculated dissociation barrier has an energy of 1.33 eV. This barrier is significantly higher than the barriers for the corresponding geometries on the clean surface and at $\theta_{CO} = 0.25$ ML.

The most stable CO adsorption geometry on Fe(100) is the hollow site with the CO bond tilted toward the Fe(100).[36] We also calculated the $H_2$ dissociation profile for this tilted CO geometry at $\theta_{CO} = 0.5$ ML on the top site with the H−H bond rotated by 45° parallel to the surface plane. We found that the $H_2$ molecule experiences an extremely large repulsion as it approaches the surface. The dissociation barrier in this case has an energy value of 2.46 eV. This barrier is a lot higher than that of the corresponding geometry with the CO molecular axis perpendicular to the surface. It is clear that when the CO is tilted on the surface at $\theta_{CO} = 0.50$ ML, dissociation would probably only take place if the CO molecules rotates to the perpendicular positions.

**$H_2$ Dissociation on the C-Covered Fe(100) Surface.** It has been shown that the tilted CO molecules on Fe(100) can readily dissociate upon heating to above 400 K.[37,38] This will result in atomic C and O on the surface. It is therefore important to also consider the effect of a C-precovered surface on $H_2$ dissociation.

***$\theta_C = 0.25$ ML.*** The resulting $H_2$ dissociation profiles on Fe(100) with $\theta_C = 0.25$ ML can be seen in Figures 5 and 6. The left profile of Figure 5 shows the dissociation profile of $H_2$ on the top site with H atoms ending up on the bridge sites. As the $H_2$ approaches the surface, it experiences a slightly stronger repulsion than what was seen for the corresponding pathway on a clean surface, but not as strong as at $\theta_{CO} = 0.25$ ML. No molecular adsorbed state can be observed. The dissociation barrier has an energy value of 0.55 eV. This barrier is almost twice as high as on the clean surface, but much lower than at $\theta_{CO} = 0.25$ ML. Once again, the two H atoms are not equivalent and the one that is the closest to the C atom will eventually move down into the hollow site right next to it, which has a more favorable adsorption energy.

The profile on the right in Figure 5 shows the $H_2$ dissociation profile on the Fe(100) surface with $\theta_C = 0.25$ ML on the top site with the H−H bond rotated by 45° parallel to the surface. In this case, the H atoms end up in the unoccupied hollow sites. The $H_2$ approaches to 2.05 Å, where it goes over a barrier of 0.16 eV to enter a molecular adsorbed state at 1.78 Å above the surface with a slightly stretched H−H bond length. The depth of the energy well of this molecularly adsorbed state is once again very shallow. The energy will increase up to the dissociation barrier with an energy value of 0.49 eV. Although this barrier is lower than that of the CO-precovered surfaces, it is still about twice as large as the lowest barrier on a clean Fe(100) surface (0.24 eV). The adsorption energy of the two H atoms in these hollow sites is −0.66 eV ($E_{ads} = -0.33$ eV per H atom).

From the previous profiles it is clear that there is also a repulsion between the C and the approaching $H_2$ molecule. We therefore also considered an off-symmetry adsorption profile similar to one we calculated at $\theta_{CO} = 0.25$ ML with the $H_2$ center of mass shifted away from the C by 0.5 Å. This profile can be seen in Figure 6. It is clear that the C−$H_2$ repulsion is significantly smaller in this case. The corresponding dissociation barrier is 0.25 eV. This is smaller than most of the barriers we calculated on the clean surface. It is quite clear that the off-symmetry sites become very important when there is another adsorbate covering the surface.

We also considered the dissociation of $H_2$ on the bridge site which is not directly next to the C. The $H_2$ reaches a dissociation barrier of 0.31 eV with a profile that looks very similar to that of the clean surface bridge site. Over the two possible hollow sites much larger repulsions were observed than that which was observed on the clean surface, indicating that the barriers will be higher than that of the clean surface hollow site.

We also considered the dissociation profile of $H_2$ directly on the preadsorbed carbon on the surface. This would directly form $CH_2$. In this case, the $H_2$ experiences an extremely strong repulsion as it approaches the C atom. The calculated barrier value is 2.20 eV for this process. This high barrier for direct $CH_2$ formation indicates that $CH_2$ would not likely be formed by direct addition of $H_2$ to the C atom and that the $H_2$ first needs to be dissociated by the iron atoms. The strong repulsion in this case would likely redirect the $H_2$ molecule to a more favorable site (e.g., off-symmetry or bridge sites).

***$\theta_C = 0.50$ ML.*** Figure 7 shows the dissociation profile of $H_2$ on the top site at $\theta_C = 0.50$ ML. The left panel of Figure 7 shows the on top dissociation pathway. Once again, all the bridge sites will have a C-atom in the hollow next to it. As the $H_2$ approaches the surface, it experiences a slightly stronger repulsion than what was seen for the corresponding pathway at $\theta_C = 0.25$ ML and the clean surface. No distinct molecular adsorbed state was observed. The resulting dissociation barrier has an energy value of 0.95 eV. The adsorption energy of the two H atoms on the bridge site is 1.78 eV ($E_{ads} = 0.89$ eV per H atom). This adsorption energy is very unfavorable and the H

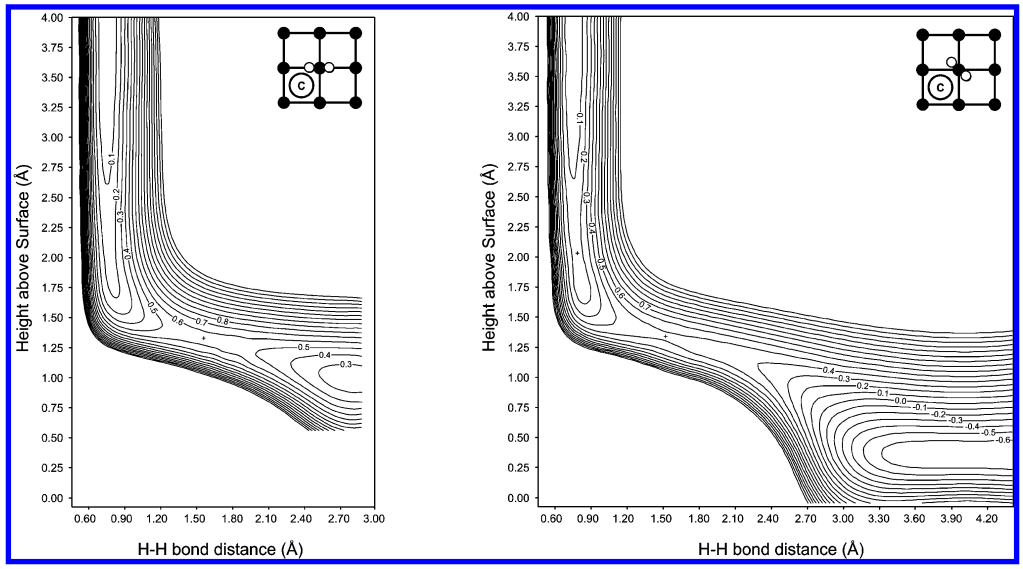


**Figure 5.** PES for $H_2$ dissociation on a $\theta_C = 0.25$ ML precovered Fe(100) surface with $H_2$ on top and rotated by 45°.

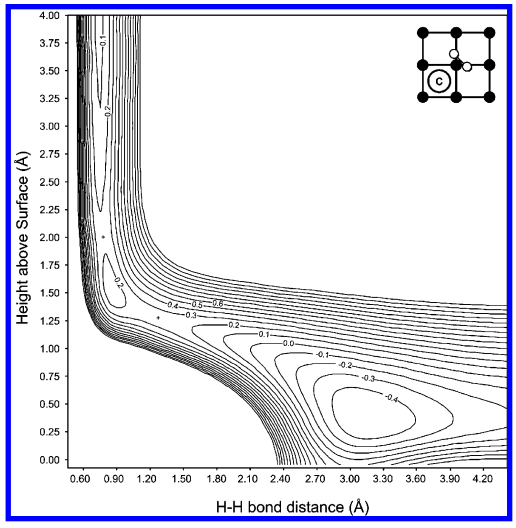


**Figure 6.** PES for $H_2$ dissociation on a $\theta_C = 0.25$ ML precovered Fe(100) surface with $H_2$ rotated by 45°. The $H_2$ center of mass is slightly moved from the high-symmetry top site.

atoms would probably be pushed into the empty hollow sites right next to them. Once again, the C−H repulsion can be seen.

The right profile in Figure 7 shows the dissociation profile of $H_2$ on the top site with the H−H bond rotated by 45° parallel to the surface plane. In this case, the H atoms end up in the two remaining hollow sites. The initial repulsion $H_2$ experiences as it approaches the surface is similar to that at $\theta_C = 0.25$ ML. No distinct molecular adsorbed state can be observed. The dissociation barrier has an energy of 0.71 eV. This barrier is higher than at $\theta_C = 0.25$ ML. The adsorption energy of the dissociated H atoms in the hollow sites is −0.78 eV ($E_{ads}$ = −0.39 eV per H atom).

Dissociation over the hollow sites and bridge sites cannot take place, since the bridge sites are blocked by the adsorbed C in the hollow sites.

**Zero-Point Corrections.** The above description considers $H_2$ as a classical particle. If we also want to consider it as a quantum particle, we have to take into account the zero-point vibrations. We have calculated the estimated minimum zero point energy perpendicular to the minimum energy pathway for selected profiles. The zero-point-corrected overall barrier values are summarized in Table 1. It is of interest to note that after the zero-point corrections have been applied, all the dissociation barriers have values that are approximately 0.1 eV lower than in the classical approach.

**Electronic Analysis.** We have calculated the Mulliken charges of the clean and precovered surfaces before the reaction with $H_2$. These estimated charges are summarized in Table 2. The clean surface has a very small projected charge per surface atom. This changes as C and CO is introduced. The C atoms have large negative charges of −0.75 $e^-$ at both coverages, while the CO molecules have cumulative charges of −0.82 $e^-$ and −0.79 $e^-$ at $\theta_{CO} = 0.25$ ML and $\theta_{CO} = 0.50$ ML, respectively.

We also calculated the LDOS for the same systems. Plots of the d-electron LDOS of the surface Fe atoms of these systems can be seen in Figure 8. These plots are all relative to the Fermi level ($E_f$) (see Table 2). It is clear that although these d-bands are different in internal shape, the center of gravity of all these bands are at approximately the same position relative to the Fermi level. The Fermi level, on the other hand, becomes lower as we introduce more C and CO to the surface. Since the d-band position does not change relative to the Fermi level, this change in the Fermi level will result in the subsequent lowering of the absolute energy of the d-bands.

The first of these electronic effects is the negative charges on the CO and C adsorbates. According to Nørskov et al.,[15] the change in reactivity toward $H_2$ is due to the interaction of the hydrogen molecule with the electrostatic field that is induced by the adlayer. A negative field is regarded as a "poison" for the dissociation reaction. This seems to fit very well our calculated charges and the accompanying increases in the barriers. The charge transfer that created the charged surface species is usually associated with a change in the Fermi level. As the Fermi level decreases, the difference in energy between the $1\sigma_g$ orbital of $H_2$ and the d-band decreases. Since the $1\sigma_g$ is a fully filled orbital, the Pauli repulsion will increase with the lowering of the Fermi level. The attractive interaction between the Fermi level and the LUMO ($1\sigma_u^*$) of $H_2$ is responsible for the weakening of the $H_2$ bond. Since a lowering in the Fermi level will increase the difference between these two electronic levels, this interaction becomes weaker. We can therefore expect a increase in the dissociation barrier of $H_2$ if the Fermi level and d-band shift to lower energies. To further illustrate this relation, we plotted the top 45° site dissociation barriers as a function of a change in the Fermi level energy relative to the

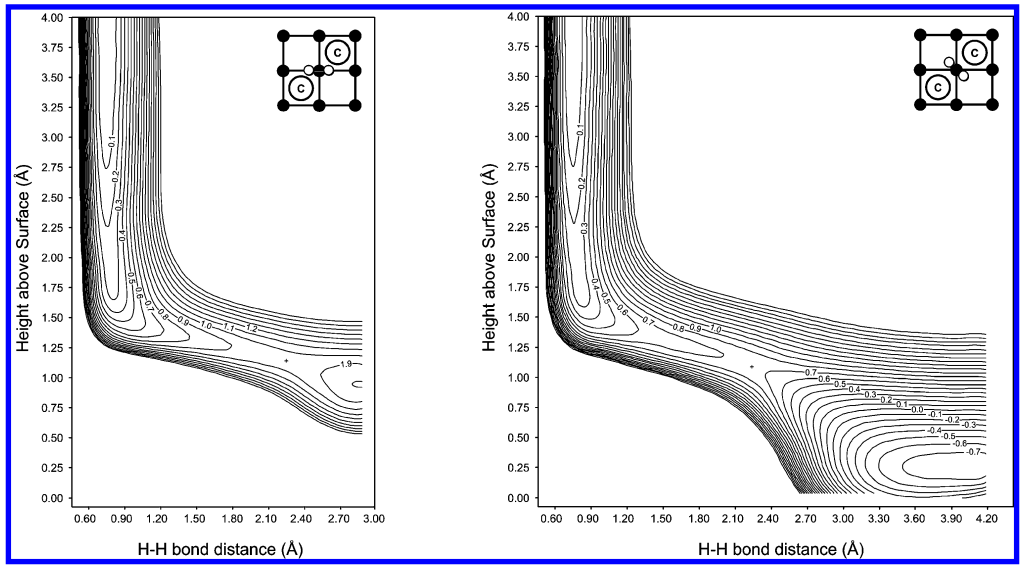


**Figure 7.** PES for $H_2$ dissociation on a $\theta_{CO} = 0.5$ ML precovered Fe(100) surface with $H_2$ on top and on top rotated by 45°.

**TABLE 2: Calculated Charges ($q$), d-Band Centers of Gravity Relative to the Fermi Level Energy ($E_d$), and the Fermi Level Energies ($E_f$) for the Clean and Precovered Fe(100) Surfaces**[a]

| system | $q_{Fe}$ | $q_C$ | $q_O$ | $E_d$ (eV) | $E_f$ (eV) |
|---|---|---|---|---|---|
| clean surface | 0.04 | | | −2.49 | −3.69 |
| $\theta_C = 0.25$ ML | 0.25 | −0.75 | | −2.53 | −3.98 |
| $\theta_C = 0.50$ ML | 0.40 | −0.75 | | −2.58 | −4.38 |
| $\theta_{CO} = 0.25$ ML | 0.25 | −0.42 | −0.40 | −2.48 | −4.51 |
| $\theta_{CO} = 0.50$ ML | 0.45 | −0.42 | −0.37 | −2.49 | −5.02 |

[a] All charges are in $e^-$ per atom.

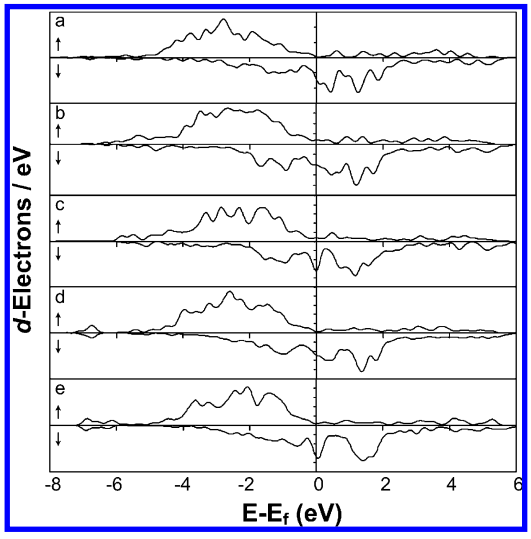


**Figure 8.** DOS plots of the spin-resolved d-bands of the surface Fe atoms for clean and precovered Fe(100) surfaces: (a) clean surface, (b) $\theta_C = 0.25$ ML, (c) $\theta_C = 0.5$ ML, (d) $\theta_{CO} = 0.25$ ML, and (e) $\theta_{CO} = 0.5$ ML.

clean surface value (Figure 9). In this view, the $H_2$ position is kept constant and the CO and C occupy a similar surface area. This obviously does not include local effects that may result in a decrease of the barrier energy (as can be seen in the resulting off-symmetry dissociation pathways). From Figure 9 it is clear that the barrier height increases as the Fermi level decreases. A linear regression of these values gave an empirical function of $E_a = -0.755E_f + 0.28$. By using this we predict that if the Fermi level of the Fe(100) surface can be increased by at least

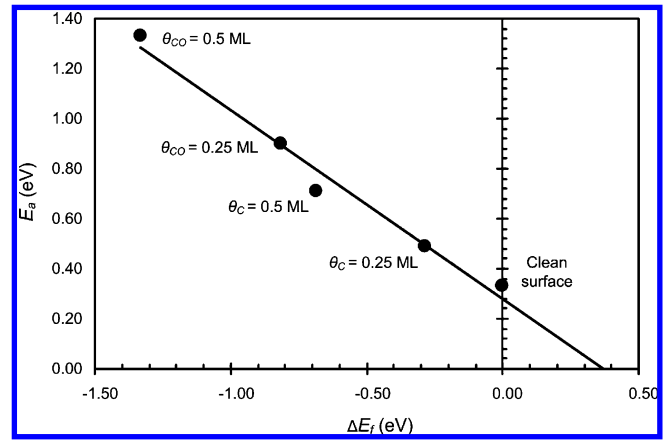


**Figure 9.** The $H_2$ dissociation barriers ($E_a$) on the on top rotated by 45° site as a function of the change in the Fermi level $\Delta E_f$.

0.37 eV (by alloying or adding an electropositive promoting adsorbate) the dissociation barrier can be decreased to 0 eV.

## Discussion

A summary of all the barriers that we have calculated is given in Table 1. If we consider the values in Table 1, it is clear that most of the barriers for dissociation of $H_2$ change due to the preadsorbed C and CO on the surface. On the clean surface the lowest calculated zero-point corrected barrier for $H_2$ dissociation is on the top site (0.16 eV). When we consider preadsorbed CO at $\theta_{CO} = 0.25$ ML, we see that the barriers for both the top and the rotated top type adsorption sites have increased significantly. An off-symmetry site has taken over the role as the lowest "late" adsorption barrier (after the "elbow-curve") for both CO and C. It is interesting to note that in both cases the bridge site adsorption barrier ("early" barrier) has not changed significantly.

When the preadsorbate coverage is increased further, the picture changes significantly. $H_2$ dissociation with $\theta_{CO} = 0.5$ ML has the lowest calculated zero-point-corrected barrier at 1.24 eV for the top 45° site, while at $\theta_C = 0.5$ ML the lowest calculated zero-point-corrected barrier energy is 0.60 eV for the top 45° site. These values are 3−6 times larger than the barriers on a clean surface. In this model these are the only available adsorption pathways at these high CO and C coverages, since

the bridge sites are effectively blocked. By being directly next to the bridge sites, adsorption on the bridge sites are also blocked due to the large CO−H and C−H repulsion at these sites. The CO and C will also block certain hollow sites for adsorption by physically occupying certain hollow adsorption sites.

The calculated increase of the dissociation barriers in the presence of C is in agreement with the effects described by the TPD experiments of Benziger and Madix.[39] They showed that carbon contamination of the Fe(100) surface reduced the surface's affinity for hydrogen. They proposed that at 200 K the initial sticking probability was reduced by an order of magnitude.

These sharp increases of the barriers at certain high-symmetry points will increase the degree of corrugation of the surface potential. This will contribute to the steering of slow moving (kinetic energy of less than $E_k \approx 0.10$ eV) $H_2$ molecules to the sites with the lower barriers (steering effect[28]). This may be a contributing factor in the case of the Fischer−Tropsch synthesis, since the average kinetic energy in the Fischer−Tropsch temperature range (500−650 K) is between 0.2 and 0.30 eV. If the kinetic energy of the hydrogen molecules is increased, this steering effect will become less effective. The favorable pathways generally seem to be the bridge sites and off-symmetry sites at coverages of 0.25 ML for both C and CO. Although the bridge sites seem favorable at a first glance, the dissociation of the $H_2$ molecule will be dynamically hampered on these sites if the $H_2$ molecules are vibrationally excited. This is due to the fact that not only is the barrier height of importance but also the position of the barrier on the PES.[40] If the barrier is "early", no translational−vibrational coupling is possible. It has been shown from molecular beam simulations that the hydrogen molecules that are not vibrationally excited have a lower probability for dissociation.[32] In the case of these bridge site profiles, no significant vibrational excitation can take place and therefore the pathway will only be available for the dissociation of molecules with a normal kinetic energy component larger than the barrier height. The other $H_2$ molecules on these sites will be reflected away from the surface.

There are therefore two important effects involved when we consider the overall view of $H_2$ dissociation in the presence of preadsorbed C or CO on the Fe(100) surface: (1) the increase in the $H_2$ dissociation barriers (due to changes in the surface electronics, like the Fermi level) and (2) the physical blocking of available adsorption sites.

If we consider the rate of hydrogen adsorption in an Arrhenius-type equation, the rate constant ($k$) of the dissociation process can be written as the product of the barrier height in the exponent ($e^{-E_a/RT}$) and a pre-exponential factor ($A$). It is clear that an increase in the activation energy of dissociation will significantly lower the adsorption rate constant (effect 1). Considering the fact that the pre-exponential factors for dissociative adsorption (order of $10^6$ $s^{-1}$) are generally significantly lower than that of surface processes (order of $10^{13}$ $s^{-1}$), the dissociative adsorption process cannot be considered to be a fast reaction. Changes to the value of the pre-exponential factor will therefore also have an impact on the rate constant. The decrease of the number of possible dissociation pathways and the physical blocking of the adsorption sites of the H atoms (effect 2) will contribute to a lower $A$ value.

At highly precovered surfaces, these two effects will result in a significant lowering of the rate constant of adsorption. Van Santen and Niemantsverdriet noted that with low pre-exponential factors, dissociative adsorption processes might already be the rate-limiting step in many catalytic cycles.[41] This might become the case for hydrogen dissociation over a highly C- or CO-covered Fe(100) surface due to the accompanying large increases in the dissociation barriers and blocking of adsorption and dissociation sites.

The implication of this for the Fischer−Tropsch synthesis is that surface hydrogen in not necessarily freely available. This hydrogen availability will depend on the effect of the other coadsorbates (like CO and C in this case) on the $H_2$ dissociation barrier.

## Conclusions

We have calculated the PES of the dissociation process of $H_2$ on a clean and on precovered Fe(100) surfaces. From the results it is clear that the presence of CO and C will block several sites for hydrogen adsorption as well as increase the hydrogen dissociation barriers. At CO and C coverages up to 0.25 ML, the main contributor to the barrier increase is the CO−H and C−H repulsion. In these cases, off-symmetry sites will play an important role to dissociate the approaching hydrogen molecules.

At coverages around 0.5 ML of CO and C, we showed that the dissociation barriers increased to more than 3 times that of the clean surface. Since the effect of the activation barrier is exponentially expressed, this will result in a significant decrease in the rate constant for the dissociative adsorption process. Another factor at this coverage is the fact that many of the hydrogen adsorption sites will be blocked, as well as the fact that the number of available possible pathways has also decreased. This will lower an already low pre-exponential factor. Overall, the rate of dissociative hydrogen adsorption will be severely hampered in the presence of a highly CO- or C-covered surface.

**Acknowledgment.** P.v.H. would like to acknowledge Sasol Technology (Pty) Ltd. for the financial support of this project.

## References and Notes

(1) Ertl, G. *J. Vacuum Sci. Technol. A* **1983**, *1*, 1247.
(2) Dry, M. E. *Catal. Today* **2002**, *71*, 227.
(3) Lundqvist, B. I.; Nørskov, J. K.; Hjelmberg, H. *Surf. Sci.* **1979**, *80*, 441.
(4) Gross, A.; Wilke, S.; Scheffler, M. *Phys. Rev. Lett.* **1995**, *75*, 2718.
(5) Gross, A. *J. Chem. Phys.* **1999**, *110*, 8696.
(6) Boszo, F.; Ertl, G.; Grunze, M.; Weiss, M. *Appl. Surf. Sci.* **1977**, *1*, 103.
(7) Burke, M. L.; Madix, R. J. *Surf. Sci.* **1990**, *237*, 20.
(8) Merrill, P. B.; Madix, R. J. *Surf. Sci.* **1996**, *347*, 249.
(9) Sorescu, D. C. *Catal. Today* **2005**, *105*, 44.
(10) Berger, H. F.; Grosslinger, E.; Rendulic, K. D. *Surf. Sci.* **1992**, *261*, 313.
(11) Ko, E. I.; Madix, R. J. *Surf. Sci.* **1981**, *109*, 221.
(12) Feibelman, P. J.; Hamann, D. R. *Phys. Rev. Lett.* **1984**, *52*, 61.
(13) Feibelman, P. J.; Hamann, D. R. *Surf. Sci.* **1985**, *149*, 48.
(14) Hammer, B. *Phys. Rev. B* **2001**, *63*, 205423.
(15) Nørskov, J. K.; Holloway, S.; Lang, N. D. *Surf. Sci.* **1984**, *137*, 65.
(16) Wei, C. M.; Gross, A.; Scheffler, M. *Phys. Rev. B* **1998**, *57*, 15572.
(17) Van Helden, P.; Van Steen, E. *J. Phys. Chem. C* **2008**, *112*, 16505.
(18) Segall, M. D.; Lindan, P. J. D.; Probert, M. J.; Pickard, C. J.; Hasnip, P. J.; Clark, S. J.; Payne, M. C. *J. Phys: Condens. Matter* **2002**, *14*, 2717.
(19) Hammer, B.; Hansen, L. B.; Nørskov, J. K. *Phys. Rev. B* **1999**, *59*, 7413.
(20) *MS Modeling 4*; Accelrys Software Inc., http://www.accelrys.com.
(21) Monkhorst, H. J.; Pack, J. D. *Phys. Rev. B* **1976**, *13*, 5188.
(22) Murnaghan, F. *Proc. Natl. Acad. Sci.* **1944**, *30*, 244.
(23) Birch, F. *Phys. Rev.* **1947**, *71*, 809.
(24) Kittel, C. *Introduction to Solid State Physics*, 7th ed.; John Wiley and Sons: New York, 1996.
(25) Kohlhaas, R.; Donner, P.; Schmitz-Pranghe, N. *Z. Angew. Phys.* **1967**, *23*, 245.
(26) Tyson, W. R.; Miller, W. A. *Surf. Sci.* **1977**, *62*, 267.

(27) Huber, K. P.; Herzberg, G. *Molecular Spectra and Molecular Structure 4: Constants of Diatomic Molecules*; Van Norstrand Reinhold Co.: New York, 1979.
(28) Gross, A.; Scheffler, M. *Phys. Rev. B* **1998**, *57*, 2493.
(29) Wilke, S.; Scheffler, M. *Phys. Rev. B* **1996**, *53*, 4926.
(30) Eichler, A.; Hafner, J.; Gross, A.; Scheffler, M. *Phys. Rev. B* **1999**, *59*, 13297.
(31) Dianat, A.; Sakong, S.; Gross, A. *Eur. Phys. J. B* **2005**, *45*, 425.
(32) Darling, G. R.; Holloway, S. *J. Chem. Phys.* **1992**, *97*, 5182.
(33) Morse, P. M. *Phys. Rev.* **1929**, *34*, 57.
(34) Mulliken, R. S. *J. Chem. Phys.* **1955**, *23*, 1833.
(35) Sanchez-Portal, D.; Artacho, E.; Soler, J. M. *Solid State Commun.* **1995**, *95*, 685.
(36) Bromfield, T. C.; Curulla Ferré, D.; Niemantsverdriet, J. W. *ChemPhysChem* **2005**, *6*, 254.
(37) Moon, D. W.; Bernasek, S. L.; Lu, J.-P.; Gland, J. L.; Dwyer, D. *Surf. Sci.* **1987**, *184*, 90.
(38) Cameron, S. D.; Dwyer, D. J. *Langmuir* **1988**, *4*, 282.
(39) Benziger, J.; Madix, R. J. *Surf. Sci.* **1980**, *94*, 119.
(40) Polanyi, J. C. *Science* **1987**, *236*, 680.
(41) Van Santen, R. A.; Niemantsverdriet, J. W. *Chemical Kinetics and Catalysis (Fundamental and Applied Catalysis)*; Plenum Press: New York, 1995.

JP909689A